Environmental Science: Atmospheres

ROYAL SOCIETY OF CHEMISTRY

PAPER

View Article Online
View Journal | View Issue



Cite this: *Environ. Sci.: Atmos.*, 2023, **3**, 717

# Pros and cons of wood and pellet stoves for residential heating from an emissions perspective†

Michael Priestley, [ac] Xiangrui Kong, [a] Xiangyu Pei,‡[a] Julia Hammes,§[a] Daniel Bäckström,[b] Ravi K. Pathak, [a] Jan B. C. Pettersson [a] and Mattias Hallquist *[a]

Biomass burning is a growing alternative to fossil fuels for power generation. Small-scale residential wood combustion introduces air pollutants to local populated areas compared to remote, large-scale facilities. Pellet fuel appliances are an alternative to log burning as they are considered more efficient; however, as emissions are not as well characterized, comparative studies to establish the potential benefits of increased pellet stove usage is required. Here we describe a distinction in optical and chemical properties of emissions from a residential pellet and a log-burning stove using state-of-the-art online measurements. Specifically, we report the first online simultaneously phase-resolved semi-volatile organic measurements from such appliances, using a Time of Flight Chemical Ionisation Mass Spectrometer with a Filter Inlet for Gas and AEROsols (FIGAERO-ToF-CIMS). Pellet particle emissions were 90% brown carbon-containing substituted mono-aromatic compounds (SMAs) whereas wood emissions contained equal black carbon (BC) and organic carbon (OC) and contained 3–55 times more poly-aromatic hydrocarbons (PAHs). Lowering pellet fuel loadings increased OC and SMA emission factors ($EF_{OC}$ and $EF_{SMA}$), therefore increasing particle mass as well as optical absorption, *i.e.* "brownness". The consequence of these EF differences is illustrated for a hypothetical national burden assuming a base case 10 : 1 log to pellet stove energy demand usage and a 'swapped' demand to simulate increased pellet stove usage. This results in net decreases of PM and BC burdens by 12% and 42% respectively but is somewhat offset by a 57% increase in OC burden. Changes in phase resolved speciated organic EFs suggest the reduction in particle burdens is somewhat offset by increases in gas burdens for some organic species, which could contribute to delayed particle burdens through secondary aerosol formation.

Received 21st March 2022
Accepted 14th February 2023

DOI: 10.1039/d2ea00022a

rsc.li/esatmospheres



## Environmental significance

An alternative to fossil fuels considered sustainable, and thus a viable replacement, is biomass combustion. Residential wood combustion has grown in popularity, increasing air pollution in populated areas. The composition and quantity of emissions can vary substantially depending on factors including appliance type and efficiency. We quantify and contrast optical and chemical properties of gaseous and particle emissions from a modern wood burning and a pellet burning stove. While still generally less polluting than the wood-burning stove in terms of particulate emissions, here we show the pellet stove emitted similar quantities of organics in the form of brown carbon, which can be exacerbated if appliance efficiencies are reduced. As a result, a hypothetical national-scale scenario based on results from the two stoves tested in this study indicated particulate matter reductions effected by swapping appliances may be modestly offset. Additionally, the pellet appliance emitted emit larger quantities of SVOCs as gases, likely increasing SOA burdens even though the POA burden is reduced.

## Introduction

Small-scale residential wood combustion (RWC) continues to increase in popularity in many European countries[1] as EU policies consider biomass burning (BB) a key technology to meet future energy targets.[2–5] RWC represents the largest source of particulate matter (PM) throughout Europe, in particular during winter.[6–8] Specifically, RWC is a significant or dominant source of primary organic aerosol (POA) and black carbon (BC), with $BC_{RWC}$ contributing to 40 000–60 000 deaths in Europe.[9,10]

[a]*Department of Chemistry and Molecular Biology, University of Gothenburg, 412 96, Gothenburg, Sweden. E-mail: hallq@chem.gu.se*

[b]*Research Institutes Sweden (RISE), Brinellgatan 4, 504 62 Borås, Sweden*

[c]*IVL Swedish Environmental Research Institute, Aschebergsgatan 44, 411 33, Gothenburg, Sweden*

† Electronic supplementary information (ESI) available. See DOI: https://doi.org/10.1039/d2ea00022a

‡ Now at College of Environmental and Resource Sciences, Zhejiang University, 310058 Hangzhou, China.

§ Now at AWA Sweden AB, Södra Hamngatan 37-41, 41106 Göteborg, Sweden.

Emissions from RWC can vary substantially from several factors to an order of magnitude, as they are highly dependent on combustion conditions, which are often dictated by fuel loadings, log size, moisture content, wood type and air supply.[11] A recent technological solution for reducing RWC emissions is the use of wood pellets as fuel rather than logs.[12,13] Pellet stoves autonomously control oxygen and fuel supplies to optimise burning conditions,[14] contrasting with less efficient, manually loaded wood log burners.[15,16] The difference in emissions between appliances is large enough that emissions are treated separately in emission inventories.[16,17] However, detailed chemical and optical measurements of emissions from these appliances are lacking, especially concerning the composition of organic carbon (OC), and is an area recommended for further investigation.[11]

POA absorbing light at 300–400 nm is called brown carbon (BrC) with similar optical and radiative properties to BC,[18] but a comprehensive understanding of its impact on climate is lacking.[19–21] The largest source of BrC in many European countries is RWC, which is an especially acute problem during the winter months and during the night.[22–24] BrC originates from lignin pyrolysis and is typically associated with less efficient combustion,[25] although secondary BrC sources are also known.[26,27] Even if a full understanding of BrC impacts on the climate are not yet understood, recent work shows the direct radiative effect of BrC is comparable, and in some instances, potentially greater than BC, *e.g.* in the tropical mid and upper troposphere.[28] Whilst global modelling efforts to include BrC for improved radiative forcing estimates are ongoing,[29] the treatment of BrC as a pollutant and contributor to poor air quality at shorter times scales and at local or regional levels is not currently considered, or specifically targeted by legislation.

Whilst many BrC constituents are harmful to human health, such as poly-aromatic hydrocarbons (PAHs) and substituted mono-aromatic compounds (SMAs), *e.g.* nitrophenol,[30,31] the full extent of BrC toxicity is unknown. These compounds are also responsible for the particle 'brownness' as they contain chromophores, *e.g.* aromatic, nitrated, multifunctional carbonyl or unsaturated moieties. Key BrC markers are known to have both gaseous and particle phase routes to formation and many of these organic constituents are semi-volatile with significant gas and particle components.

Detailed analysis of BrC constituents is commonly performed offline by analysing filter samples using separation techniques such as gas chromatography (GC)[32] and high performance liquid chromatography (HPLC).[33] Online measurements of residential wood burning emissions reported using aerosol mass spectrometer (AMS) give bulk aerosol properties,[15] and ambient measurements frequently return biomass burning factors when used in conjunction with positive matrix factorisation (PMF),[34] although little information on the chemical composition of the BrC is derivable.

Trace compounds from biomass burning can be measured online in the gas phase with mass spectrometric techniques, *e.g.* proton-transfer mass spectrometry (PTR).[35,36] Iodide chemical ionisation mass spectrometry (CIMS) has been used to quantify low molecular weight BrC components such as N containing aromatic compounds.[37–40] Time of Flight Chemical Ionisation Mass Spectrometer with a Filter Inlet for Gas and AEROsols (FIGAERO-ToF-CIMS)[41] has been demonstrated to measure gas and particle phase BrC components from ambient biomass burning in China.[39,42] Chamber studies of BrC formed from nitration of unsaturated heterocycles, which combined optical, HPLC and iodide-CIMS measurements, showed that complementary optical, gas and particle phase measurements are a suitable combination to characterise BrC.[43]

Here, for the first time, we present simultaneous, online measurements of a range of organic compounds, including SMAs, in both particle and gas phases from a wood burning stove and a pellet burning stove, using a FIGAERO-ToF-CIMS.[41,44] We describe differences in gaseous and particle emission factors (EFs) and optical and chemical properties of particle emissions from these two RWC appliances using state-of-the-art, online instrumentation. Contrasting the appliances under different operating conditions to represent a range of combustion efficiencies, we compare the effect of OC composition on optical absorption and use a case scenario analysis to evaluate potential differences in a hypothetical annual emission burden on a generalised, national scale. The phase partitioning of the OC measured here by FIGAERO-ToF-CIMS will be presented in a future publication.

## Materials and methods

The experiments were conducted at the Research Institutes of Sweden (RISE) Combustion Laboratory, Borås, Sweden.

### Appliances and fuels

A 2006 report[16] using survey data shows that 695 000 individual fireplaces were shared amongst 585 000 properties in Sweden. Of those, 44% were wood burning stoves, 23% were open fireplaces, 23% masonry stoves, 14% heat-accumulating ovens and 12% were kitchen stoves. More than half of the appliances were installed before 1991, making them over 15 years old at the time. An estimated 30 000 pellets stoves existed in Sweden for the year 2018 with approximately 2000 sold every year [17].

The ten-year-old pellet stove used in this study had a claimed nominal energy output of 3–10 kW with an 83% heating efficiency, according to the appliance manual. This model is produced by a leading European manufacturer and was operated according to factory settings to simulate real-world usage. The wood pellet fuel (6 mm, Scandbio[45]) is manufactured from logging industry waste wood without any additives. The pellets have an ash content $\leq$0.5% (w/w) and moisture content of 6–8% (w/w, dry basis) and are designed for use in commercial and residential buildings. Pellets were introduced to the combustion chamber automatically and a constant burn condition was held throughout the experiment which typically lasted 6 to 8 hours. Two load settings were investigated. The low load fuel consumption rate of 0.69 kg per hour is designed to maintain a temperature of 100 °C (as measured at the chimney bottom) and the high (full) load rate of 1.16 kg per hour represents maximized appliance usage.

The pellet stove was compared with a popular, contemporary wood log stove of similar size with a claimed nominal energy output of 6 kW, and an 86% heating efficiency, according to the appliance manual. Two wood fuels were used; spruce, with 19.6% moisture content (dry basis); and birch with the bark removed, with 17.0% moisture content (dry basis). The wood logs were approximately 27 cm long and weighed 0.7 kg each. Their placement in the combustion chamber was standardized by stacking two logs in a T shape one on top of the other, according to the manufacturer's recommendations. A 2.1 kg load was used for the first batch of the day and then 1.4 kg for the batches thereafter. The air supply to the log stove was fully opened after loading and then reduced to 50% after three minutes, in line with the manufacturer's recommendations. The cycle was repeated approximately every 50 minutes for a total of 6 to 8 cycles.

### Iodide FIGAERO-ToF-CIMS

A FIGAERO-ToF-CIMS was deployed to measure gaseous and particle phase organic species, including SMAs, using iodide ($I^-$) reagent ions. The instrument has been described in detail elsewhere,[41,44,46] here we describe the specific details related to its setup for these measurements. 2.2 standard litres per minute (slm) of $N_2$ flowed over a vial containing methyl iodide ($CH_3I$), which is emitted through a critical orifice before it passes through a $^{210}Po$ source into the ion molecule reaction region (IMR) to generate the $I^-$ ions. The IMR was held at 180 mbar by a scroll pump (Agilent SH-112) and the short-segmented quadrupole (SSQ) was held at a pressure of 1.80 mbar by a scroll pump (Triscroll 600). 30 standard cubic centimetres per minute (sccm) $N_2$ passed over a vial containing perfluoro-pentanoic acid (PFPA) from which a critical orifice controlled its emission. $NO_2^-$, $NO_3^-$, $I^-$, $IH_2O^-$, $I{\cdot}CH_2O_2^-$, $I{\cdot}HONO^-$, $I{\cdot}HNO_3^-$, $I_2^-$, $I_3^-$, PFPA iodide adduct and PFPA dimer were used to mass calibrate the instrument covering a mass range of 46–527 $m/z$. The average resolution (m $dm^{-1}$) was 2840 at 173 $m/z$ and 3000 at 527 $m/z$.

The FIGAERO-ToF-CIMS particle sample from the spruce fuel experiment occurred at a lower modified combustion efficiency (MCE) (0.9519 ± 0.0374) than the average cycle, whereas the birch FIGAERO-ToF-CIMS sample occurred at a period of higher MCE (0.9938 ± 0.0035) than average (Fig. S1†). As combustion condition is more important than wood fuel type for emission profiles,[16] we use the two FIGAERO samples to constrain upper and lower limits of wood emissions which provide a good comparison with the low load (MCE = 0.9674 ± 0.0106) and high load (MCE = 0.9951 ± 0.0009) pellet combustion efficiencies. FIGAERO derived EFs reflect this distinction. As the pellet MCEs are constant, the timing of the particle phase FIGAERO sampling was not crucial (Fig. S1†). See ESI† for further details of sensitivities, sampling, calibrations, background and FIGAERO cycle information.

### Dilution tunnel

Emissions were directed through a dilution tunnel (Norwegian Standard NS3058-1 (ref. 47)) where the draft of ambient air determines the dilution factor (Fig. S2†). For the pellet experiments this was 9.4. During FIGAERO-ToF-CIMS sampling, for the birch the dilution factor was 24.5 ± 0.1 (to one standard deviation, 1$\sigma$) and for the spruce it was 18.8 ± 3.0. For a full combustion cycle, these dilution factors increase to 24.9 ± 2.8 for the birch and 22.3 ± 2.3 for the spruce (see Table 1 for details). The diluted emissions are then further diluted by an ejector dilutor with a factor of 8.6. Wall losses of the entire system were estimated as 20% according to previous experiments.[40]

### Mono-substituted aromatic compounds (SMAs) – definitions and quantification

Aromatic compounds are identified from FIGAERO-ToF-CIMS data in two ways. Firstly, identifying compounds previously reported in the literature.[32,33,48] This method identifies 66 compounds across all experiments. Secondly, from chemical formulae that have a double bond equivalent (DBE) ≥4 and carbon numbers ≥6.[49] This method identifies 10 s–100 s of aromatic compounds for each experiment. We use the conservative estimate of the literature reported method for identifying SMAs, rather than the molecular formula-based approach to ensure as great a confidence in identification as possible and to not overestimate any effects of incorrectly identified SMAs. The DBE defined SMAs are not discussed further but are represented in Fig. 1 for comparison purposes. Assignments of molecular identities to formulae are tentative and should be treated with caution, although the majority of those discussed here have previously been identified and measured by this technique in both the lab and field giving a higher degree of confidence in their assignments. These are summarised in Table S1 of the ESI.†

### Offline PAH measurements

Sampling of PAHs from the dilution tunnel was performed collecting emissions in adsorption tubes by flowing 1 slm for 5 minutes after the third minute for the wood cycles and during steady state combustion for the pellets. The sampling for the wood occurred after the air supply was reduced by 50% and coincides with the maximum production of SVOC/PAH emission. Sample analysis was performed by gas chromatography mass spectrometry (GC-MS). These are summarised in Table S2 of the ESI.†

### Complimentary online measurements

$CO_2$ (Rosemount Analytical XSTREAM), CO (Rosemount Analytical XSTREAM), $O_2$ (M&C PMA10) and total hydrocarbons (THC, JUM FID VE5) were measured in the flue stack. $CO_2$, CO, NO and $O_2$ (Horiba PG350) were measured in the dilution tunnel. The ratio of measured gases at these two places was used to calculate the initial dilution factor described earlier. A scanning mobility particle sizer (SMPS; TSI Inc., EC 3080, DMA 3081) and condensation particle counter (CPC 3010, TSI Inc.), were used to derive particle mass (PM), number and mobility diameters within a range of 0.010–0.478 μm, assuming spherical particles and a density of 1.2 g $cm^{-3}$. SMPS size ranges were extended from 478 nm to 2594 nm by fitting Gaussians for the

Table 1 Appliance properties, optical properties and emission factors (EFs) from the pellet stove and wood-burning stove. EFs are reported on per fuel mass and useful energy delivered basis. Variability for the appliance, optical and core chemical properties are reported to 1$\sigma$, variability for FIGAERO-ToF-CIMS derived measurements are a 30% error in calibration factors. Energy contents of the wood logs used in the EF calculations were 5.3 kW h kg$^{-1}$ (ref. 67) and 4.7 kW h kg$^{-1}$ for the pellets,[45] accounting for differences in moisture contents. The carbon fraction of the fuels is assumed 0.5. EF calculations are described in the text and ESI

| | | | | | Birch | | Spruce | |
|---|---|---|---|---|---|---|---|---|
| Property | Measurement | Unit | Pellets high load | Pellets low load | FIGAERO sample | Whole wood cycle | FIGAERO sample | Whole wood cycle |
| Combustion | Temperature (chimney bottom) | °C | 152 ± 8 | 98 ± 1 | 265 ± 5 | 261 ± 14 | 236 ± 15 | 284 ± 13 |
| | MCE | — | 0.9951 ± 0.0009 | 0.9674 ± 0.0106 | 0.9938 ± 0.0035 | 0.9758 ± 0.026 | 0.9519 ± 0.0374 | 0.9615 ± 0.0218 |
| | Dilution factor (tunnel) | — | 9.4 | 9.4 | 24.5 ± 0.1 | 24.9 ± 2.8 | 18.8 ± 3.0 | 22.3 ± 2.3 |
| Optical | AAE | — | 3.5 ± 0.4 | 3.1 ± 0.1 | 1.0 ± 0.1 | 0.9 ± 0.1 | 2.1 ± 0.8 | 1.0 ± 0.6 |
| | $MAC_{405}$ | m$^2$ g$^{-1}$ | 2.7 ± 0.9 | 11.5 ± 6.6 | 2.1 ± 1.0 | 6.2 ± 11.0 | 67.0 ± 67.4 | 33.8 ± 27.4 |
| | $MAC_{781}$ | m$^2$ g$^{-1}$ | 0.3 ± 0.1 | 1.4 ± 0.7 | 1.1 ± 0.5 | 3.1 ± 5.1 | 35.3 ± 32.4 | 11.3 ± 10.3 |
| Emission factors | $CO_2$ | kg kg$^{-1}$ | 1.81 ± 0.19 | 1.77 ± 0.27 | 1.82 ± 0.06 | 1.81 ± 0.62 | 1.73 ± 0.65 | 1.79 ± 0.52 |
| | | mg MJ$^{-1}$ | 126 519 ± 13 516 | 123 065 ± 18 510 | 95 562 ± 3413 | 110 068 ± 37 713 | 105 556 ± 39 621 | 108 815 ± 31 951 |
| | CO | mg kg$^{-1}$ | 10 853 ± 2455 | 39 259 ± 7621 | 5437 ± 3788 | 15 759 ± 14 364 | 55 453 ± 19 523 | 28 579 ± 18 342 |
| | | mg MJ$^{-1}$ | 757 ± 171 | 2737 ± 531 | 331 ± 231 | 960 ± 875 | 3379 ± 1190 | 1742 ± 1118 |
| | THC | mg kg$^{-1}$ | 812 ± 204 | 4778 ± 1216 | 534 ± 248 | 1470 ± 2959 | 11 237 ± 9123 | 1742 ± 1118 |
| | | mg MJ$^{-1}$ | 57 ± 14 | 333 ± 85 | 33 ± 15 | 90 ± 180 | 685 ± 556 | 121 ± 244 |
| | PM | mg kg$^{-1}$ | 462 ± 92 | 1411 ± 759 | 515 ± 226 | 592 ± 749 | 2512 ± 4856 | 484 ± 7547 |
| | | mg MJ$^{-1}$ | 32 ± 6 | 98 ± 53 | 31 ± 14 | 36 ± 46 | 153 ± 296 | 30 ± 460 |
| | OC | mg kg$^{-1}$ | 220 ± 56 | 638 ± 394 | 149 ± 77 | 170 ± 237 | 689 ± 1391 | 196 ± 7547 |
| | | mg MJ$^{-1}$ | 15 ± 4 | 44 ± 53 | 9 ± 5 | 10 ± 14 | 42 ± 85 | 12 ± 460 |
| | BC | mg kg$^{-1}$ | 42 ± 60 | 221 ± 239 | 239 ± 90 | 284 ± 326 | 1260 ± 2352 | 206 ± 1748 |
| | | mg MJ$^{-1}$ | 3 ± 4 | 15 ± 17 | 15 ± 5 | 17 ± 20 | 77 ± 143 | 13 ± 107 |
| | Sum PAHs | mg kg$^{-1}$ | 4 ± 0 | 7 ± 0 | — | 17 ± 0 | — | 172 ± 0 |
| | | mg MJ$^{-1}$ | 0 ± 0 | 1 ± 0 | — | 1 ± 0 | — | 10 ± 0 |
| Emission factors (FIGAERO) | Levoglucosan, $C_6H_{10}O_5$, particle (gas) | mg kg$^{-1}$ | 16.46 ± 4.94 (0.20 ± 0.06) | 24.6 ± 7.40 (3.50 ± 1.10) | 26.9 ± 8.1 (0.10 ± 0.00) | — | 49.4 ± 14.8 (0.00 ± 0.00) | — |
| | | mg MJ$^{-1}$ | 1.15 ± 0.34 (0.01 ± 0.00) | 1.72 ± 0.52 (0.24 ± 0.07) | 1.64 ± 0.49 (0.01 ± 0.0) | — | 3.01 ± 0.90 (0.00 ± 0.00) | — |
| | Sum FIGAERO organics, particle (gas) | mg kg$^{-1}$ | 29.0 ± 8.70 (20.9 ± 6.30) | 65.7 ± 19.7 (84.4 ± 25.3) | 46.1 ± 13.8 (8.20 ± 2.50) | — | 81.5 ± 24.5 (14.7 ± 4.4) | — |
| | | mg MJ$^{-1}$ | 2.02 ± 0.61 (1.46 ± 0.44) | 4.58 ± 1.37 (5.88 ± 1.76) | 2.81 ± 0.84 (0.50 ± 0.15) | — | 4.97 ± 1.49 (0.90 ± 0.27) | — |
| | Sum substituted aromatics (literature definition, $n$ = 19), particle (gas) | mg kg$^{-1}$ | 3.12 ± 0.94 (4.19 ± 1.26) | 11.8 ± 3.60 (15.9 ± 4.80) | 0.61 ± 0.18 (0.51 ± 0.15) | — | 2.28 ± 0.69 (0.44 ± 0.13) | — |
| | | mg MJ$^{-1}$ | 0.22 ± 0.07 (0.29 ± 0.09) | 0.83 ± 0.25 (1.11 ± 0.33) | 0.04 ± 0.01 (0.03 ± 0.01) | — | 0.14 ± 0.04 (0.03 ± 0.01) | — |

wood experiments as measurements did not capture the full range of particle sizes. The scan time of the SMPS was 120 seconds. This increased particle mass estimations by 10% for birch and 5% for spruce (described later). An aerodynamic aerosol classifier (AAC) was used to assess morphological properties as a function of particle size and a thermodenuder (TD) was used periodically to heat particles to 400 °C. The residence time through the TD was 96 seconds. The TD was used qualitatively to observe changes in particle volume which does not require assumptions of equilibrium or the use of a kinetic model.

Measurements of CO and $CO_2$ allow for the calculation of the modified combustion efficiency (MCE, eqn (1)).[50] This is commonly calculated for ambient biomass burning measurements to describe the phase of burning and to reconcile with emission factors.

$$\mathrm{MCE} = \frac{\Delta \mathrm{CO}_2}{\Delta \mathrm{CO} + \Delta \mathrm{CO}_2} \quad (1)$$

Here we calculate MCE to compare efficiencies of different appliances used under different settings. As these appliances are designed to combust fuel efficiently, it is expected that the MCE values will be very high. Flue temperature was measured at the chimney bottom and chimney top.

### Optical measurements

A Photo Acoustic Soot Spectrometer (PASS-3) measured optical absorption at 401 nm and 781 nm to assess the relative contributions from BC[51,52] and OC (BrC). Based on the ratio of absorbances at different wavelengths, the Absorption Ångström Exponent,[53] a measure of the wavelength dependence of the absorption, was calculated as:

$$\mathrm{AAE} = -\frac{\ln(b_{\mathrm{abs}\lambda_1}/b_{\mathrm{abs}\lambda_2})}{\ln(\lambda_1/\lambda_2)} \quad (2)$$

where $\lambda_1$ and $\lambda_2$ are the wavelengths of the light absorbed, and $b_{\mathrm{abs}_{\lambda_1}}$ and $b_{\mathrm{abs}_{\lambda_2}}$ are the corresponding absorbances. The fraction of BrC was calculated by assuming only BC contributes to the absorption at 781 nm, *i.e.* $\mathrm{AAE}_{\mathrm{BC}} = 1$.[53,54] The mass absorption cross section (MAC, absorption normalised to particle mass)[55] provides a comparable measure of the intensity of absorption and is calculated by dividing the absorbance ($b_{\mathrm{abs}_\lambda}$) with the particle mass concentration (PM), derived from the SMPS (described in the particle mass quantification section).

$$\mathrm{MAC}_\lambda = \frac{b_{\mathrm{abs}_\lambda}}{\mathrm{PM}} \quad (3)$$

Using these optical properties, it is possible to estimate the aerosol mass fraction that originates from the organic fraction (OC) and refractory fraction (BC). We assume all absorption at 781 nm ($b_{\mathrm{abs}_{781}}$) is due to BC only and thus the fraction of $b_{\mathrm{abs}_{405}}$ caused by BC is calculated by rearranging eqn (2) as:

$$b_{\mathrm{abs}_{405_{\mathrm{BC}}}} = \mathrm{e}^{\ln\left(b_{\mathrm{abs}_{781}}\right)+\ln\left(\frac{781}{405}\right)} \quad (4)$$

Absorption due to the organic fraction is equal to the remainder of absorption at 405 nm.

$$b_{\mathrm{abs}_{405_{\mathrm{Org}}}} = b_{\mathrm{abs}_{405_{\mathrm{total}}}} - b_{\mathrm{abs}_{405_{\mathrm{BC}}}} \quad (5)$$

### Particle mass quantification

The BC mass concentration (BC) is calculated from its corresponding optical absorption fraction by rearranging the definitions of MAC at 405 nm for the BC and total PM (eqn (6) and (7)). Here we refer to BC but recognise this is more accurately defined as equivalent black carbon (eBC).[56] For simplicity, the abbreviation BC is used in place of eBC. The difference between BC and PM is assumed to be the remaining organic mass measurements (OM, eqn (8)). This assumption ignores contributions from inorganic salts.

$$\frac{\mathrm{MAC}_{405_{\mathrm{BC}}}}{\mathrm{MAC}_{405_{\mathrm{PM}}}} = \frac{b_{\mathrm{abs}_{405_{\mathrm{BC}}}}/\mathrm{BC}}{b_{\mathrm{abs}_{405_{\mathrm{total}}}}/\mathrm{PM}} \quad (6)$$

$$\mathrm{BC} = \mathrm{PM}\frac{b_{\mathrm{abs}_{405_{\mathrm{BC}}}}}{b_{\mathrm{abs}_{405_{\mathrm{PM}}}}}\frac{\mathrm{MAC}_{405_{\mathrm{PM}}}}{\mathrm{MAC}_{405_{\mathrm{BC}}}} \quad (7)$$

$$\mathrm{OM} = \mathrm{PM} - \mathrm{BC} \quad (8)$$

Total PM is estimated using the SMPS measurement of volume and then multiplied by an assumed effective density of 1.2 g $\mathrm{cm}^{-3}$. This was considered a reasonable value as BB particles at low mobility diameters have been measured as 1.15 $\pm$ 0.23 g $\mathrm{cm}^{-3}$, attributed to fractal black carbon[57] and effective densities of 1.19 $\pm$ 0.05 g $\mathrm{cm}^{-3}$ for BrC particles have been reported elsewhere.[58] However, as the morphology and composition of the emissions are distinct, this assumption is a limitation. The OC : OM ratio of 1.8 for biomass burning aerosol[59] was used to derive OC from OM.

It is difficult to verify these OC mass concentration estimations, as no other online measurements of OC were made. However, comparisons of mass concentrations derived from SMPS measurements with other methods of quantification have been demonstrated to show good agreement where accurate effective densities were used. Bougiatioti *et al.*[60] compared Aerosol Chemical Speciation Monitor (ACSM) and BC measurements with SMPS derived mass concentrations for an ambient wild fire study and found good agreement between measurements, although this treatment included ammonium sulfate in the effective density calculation and a significant sulfate fraction of 19% was measured by the ACSM. Bau *et al.*[61] showed mass concentrations derived from SMPS data were in good agreement ($R^2 \sim 0.9$) compared to gravimetric and chemical analyses when analysing mass loadings of 20–1000 μg $\mathrm{m}^{-3}$ of elemental carbon generated using carbon electrodes from a spark-discharge generator.

### Emission factor calculations

Emission factors (EFs) were calculated from online measurements, in units of g $\mathrm{kg}^{-1}$ of fuel burned[13,62–65] as well as in terms of useful energy delivered, g $\mathrm{MJ}_{\mathrm{delivered}}{}^{-1}$ (hereafter g $\mathrm{MJ}^{-1}$), see

eqn (9). Firstly, the excess concentration of species $X_i$ is divided by the sum of the carbon containing species in the emission[66] and multiplied by carbon fuel content, $F_C$, which is assumed to be 0.5 for all fuels. For PM and THC, we assumed a molecular formula of $C_3H_8$. Organic carbon (OC) was derived from OM using the OC : OM ratio of 1.8 for biomass burning aerosol.[59]

$$EF_{X_i} = \frac{\Delta X_i}{\Delta C_{CO_2} + \Delta C_{CO} + \Delta C_{THC} + \Delta C_{OC} + \Delta C_{BC}} F_C \quad (9)$$
$$EC_F \times 3.6\ \left(MJ\ kW^{-1}\ h^{-1}\right) \times E_A$$

EFs were converted from g $kg^{-1}$ to g $MJ^{-1}$, according to eqn (9), using the energy contents of the fuels, $EC_F$, and heating efficiencies of the appliances, $E_A$. $F_c$, $EC_F$ and $E_A$ were not measured directly but assumed. The variation in $F_c$, $E_{CF}$ and $E_A$ for the fuels use here are on the order of fractions to a few percent (see associated references), which is much lower than the measurement variability. $EC_F$ of the wood logs was assumed to be 5.3 kW h $kg^{-1}$ (ref. 67) and 4.7 kW h $kg^{-1}$ was assumed for the pellets,[45] accounting for differences in reported moisture contents. $E_A$ values were not measured, they were instead taken from the appliance manufacturers manuals. This was 86% for the wood stove and 83% for pellet stove. Of the assumed variables in eqn (9) (rather than measured variables), $E_A$ is probably the largest source of error and is likely over estimated. This overestimation would yield lower EFs and so provides a low estimate of $EF_{X_i}$.

The emissions from the pellet stove were constant for a given loading. For both loadings we used a three-hour time period over which the EFs were integrated, which is more than enough time to provide an accurate, representative measurement. The emissions from the log stove displayed emissions cycling in which there is large variability. In order to reduce uncertainties from this variability, EFs were calculated using average values from six or seven cycles for the spruce and birch cases respectively. For the wood log cases, these averaged values are reported in Table 1 under the sub heading whole wood cycle. For the adjacent columns subtitled FIGAERO sample, see the description of sampling in the Iodide FIGAERO-ToF-CIMS section. Emission factors are shown in Fig. 1.

### Hypothetical national burdens scenario

In order to contextualise potential impacts of the emissions from the two appliances, we perform a hypothetical national

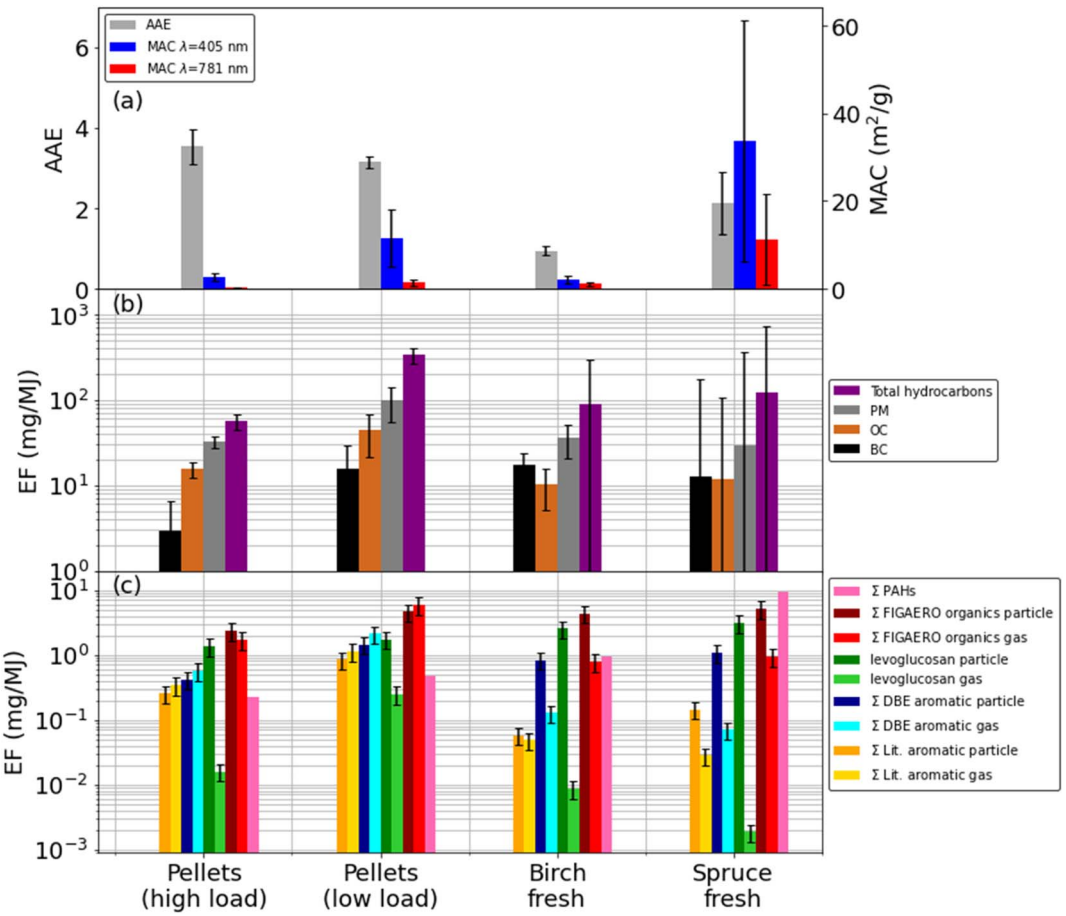


Fig. 1 (a) Summary of median AAEs and MACs. (b) Emission factors of core measurements THC, PM, OC and BC during FIGAERO sampling in units of mass per useful energy delivered. (c) Emission factors of FIGAERO measurement species and PAHs. Error bars indicate 1 standard deviation of the variability. All measurements were made in the dilution tunnel except total hydrocarbons and PAHs, which were measured in the flue. Emission factors were calculated using the dilution tunnel volumetric flow rate specific to each case.

 

burden scenario analysis where we present total, national scale, mass burden estimates for the quantified pollutants, by multiplying emission factors with estimated activities. As a base case we use a wood stove national energy consumption of 7.0 PJ and for the pellet stove, 0.7 PJ.[68] These energy consumption values are then swapped to simulate a transition towards a majority use of pellet boilers.

The EFs were combined to reflect a more realistic case assuming 90% 'good' combustion and 10% 'bad' combustion as elsewhere.[68] The 10% bad combustion criteria referenced here is based on an assumption of user behaviour rather than on data and is termed "expected behaviour" by the authors of that study. Additionally, a worst case 20% bad combustion scenario termed "worse than expected" and best case 0% bad combustion scenario termed "good combustion" were used to produce a range of realistic results. Here we use the 10% bad combustion or, "expected behaviour" scenario as a basis for our national burden scenario. Here, instead of weighting 'typical EFs', we use the efficient high pellet load EFs for the 'good' case and less efficient low pellet load for the 'bad' case. For the wood stove, birch is assumed the 'good' case as it was the most efficient, and spruce the 'bad' case, as it was less efficient.

This analysis uses emission factors presented in this manuscript only, *i.e.*, derived from these two individual appliances. Additionally, the energy swap scenario may represent an unrealistically large transition to pellet use from wood log combustion. As such, this analysis is not meant to provide evidence for a realistic policy implementation but is an exercise in contextualising our results and demonstrating hypothetical impacts, rather than presenting definitive burdens or burdens for any specific country. A more detailed study using a more accurate representation of RWC appliances, and a more realistic scenario would be beneficial to appreciate the true impact of the emission factors derived here, however such a comprehensive study is beyond the scope of this manuscript.

# Results and discussion

For all measured gases and aerosols, the pellet stove produced stable conditions compared to the wood stove, which displayed cycles determined by burning phases and refuelling, which is typical of log burning appliances.[69] This is best exemplified by the MCE time series (Fig. 2). Regarding the pellet stove, combustion conditions remain constant throughout the experiment, whereas for the logs, as temperature reduces after most of the fuel is consumed, combustion is poor, and MCE reduces. New logs must also be heated before they combust and before high MCEs are reached again. Heterogeneous combustion conditions, caused by, *e.g.*, shape or density differences in the wood, colder regions in the combustion chamber, or regions with reduced airflow, mean the average MCE may never be as high as for the homogenous pellet fuel. Reproducibility of the wood-burning emissions cycles is high, apart from during start-up from cold conditions and at the end of the birch-log burning time series where a larger (3 kg) log was used.

Typical concentrations of OC during sampling were ~1000 μg $m^{-3}$ during the high MCE birch and pellet high load experiments (Table S3†). This increased to ~2500 μg $m^{-3}$ for the low pellet loading and ~5700 μg $m^{-3}$ for the fresh spruce experiment. The wood log measurements were made at higher dilution rates than the pellet measurement, as described in the dilution tunnel section. The FIGAERO sampling time of 5 minutes at 2 slm then provided between 20–50 μg deposited onto the filter for analysis.

### Chemical composition of emissions

For the high MCE birch and high load pellet cases, $EF_{CO_2}$ are 1.82 ± 0.06 kg $kg^{-1}$ and 1.81 ± 0.19 kg $kg^{-1}$ respectively, which are greater in magnitude than the lower MCE cases of spruce and the low pellet load, where $EF_{CO_2}$ were 1.73 ± 0.65 kg $kg^{-1}$ and 1.77 ± 0.27 kg $kg^{-1}$ respectively. In these figures the high variability for the wood log cases, due to the cycling, is also seen. Correspondingly, the $EF_{CO}$ for the high MCE cases are lower, with 10.8 ± 2.4 g $kg^{-1}$ for the high pellet load and 15.8 ± 14.4 g $kg^{-1}$ for the birch case compared with 39.2 ± 7.6 g $kg^{-1}$ for the low pellet load and 55.4 ± 19.5 g $kg^{-1}$ for the spruce case (Fig. 1 and Table 1).[30,63,64,70–72] The trend of high MCE birch and high load pellet cases producing less particulate material is reflected in the PM EFs and subsequently derived EFs for BC and OC. See Table 1 for details.

The $EF_{BC}$ for the low load pellet case and wood logs (206 ± 1750 mg $kg^{-1}$ to 284 ± 326 mg $kg^{-1}$) are comparable to literature values[59,63,73] whilst the high load pellet case is five to seven times lower (42 ± 60 mg $kg^{-1}$). Pellet $EF_{BC}$ of these magnitudes have been reported elsewhere for both pellet and wood log burning stoves.[73,74] High BC EFs indicate fuel rich, oxygen poor environments. This is counter-intuitive for the low loading pellet case, as it is expected that when the fuel loading is decreased, the fuel to oxygen ratio decreases and the environment is more oxygen rich. However, for these appliances, air injection is controlled autonomously. This suggests that at lower loadings, the air injection into the combustion chamber was not optimal, thus creating a fuel rich environment, even at lowered fuel loadings.

$EFs_{OC}$ also broadly agree with literature values[59,63,75] for all appliances, although here, pellet $EF_{OC}$ of 220 ± 56 mg $kg^{-1}$ for the high loading and 638 ± 394 mg $kg^{-1}$ for the low loading, are generally greater than the birch $EF_{OC}$ (170 ± 237 mg $kg^{-1}$) and spruce (196 ± 7550 mg $kg^{-1}$) cases. The low pellet load $EF_{OC}$ is noticeably larger than all other $EF_{OC}$, although the wood log $EFs_{OC}$ demonstrate extremely high variabilities of between four to 38 times their average values. The low pellet load $EF_{OC}$ is also much larger than those used elsewhere to calculate RWC impacts.[68] As these EFs are derived from optical, online measurements rather than the gravimetric, offline filter-based measurements, there is the potential that volatile compounds that would otherwise evaporate from the filter before measurement may instead be captured here, providing larger than typical values. The variabilities reported for the wood logs EFs are high which reflects the entire combustion cycle.

Offline GC-MS detects only three of 16 PAHs (Table S2†) in the pellets and birch cases and at relatively low abundances, *i.e.* 0.006% of total PM. In contrast, all 16 are identified in the spruce case and at much higher magnitudes, 0.04% of PM.

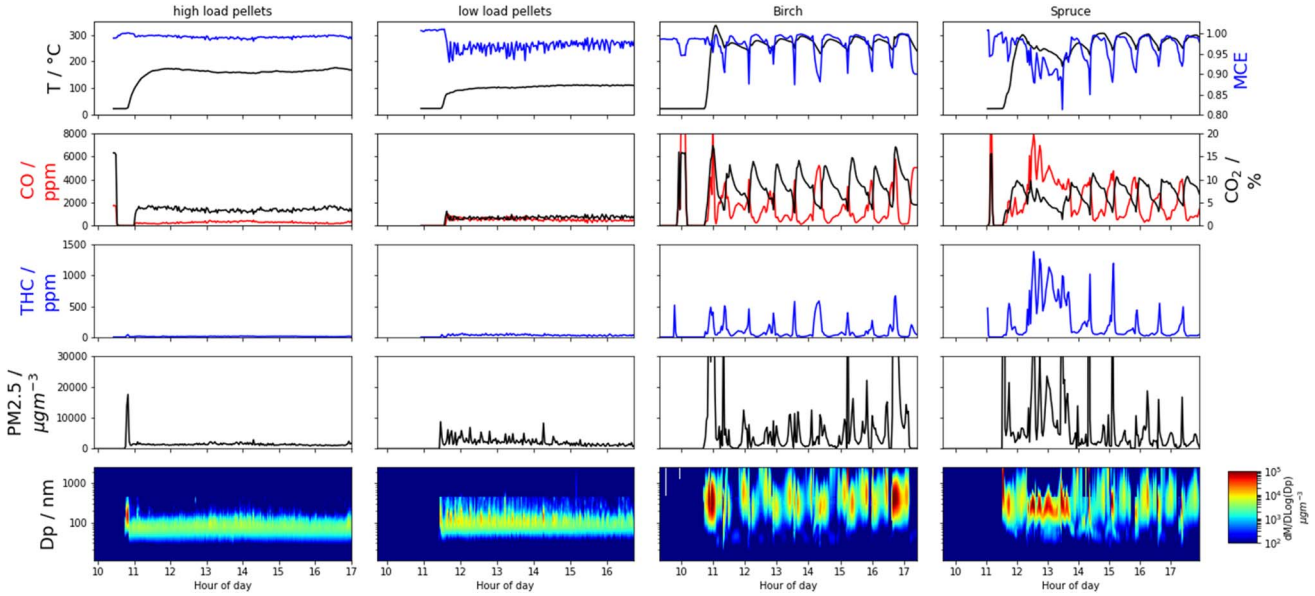


Fig. 2 Time series from the high and low load pellet, birch and spruce experiments. In rows: first row, chimney temperature† (bottom) and modified combustion efficiency† (MCE); second row, CO† (ppm) and $CO_2$† (%); third row, total hydrocarbon† (ppm); fourth row, mass concentration of PM* ($\mu m^{-3}$); fifth row, particle size distribution* (nm). † measured in chimney, * measured in the dilution tunnel.

## Morphological properties of PM

The organic mass (OM) fraction of total PM measured for the pellets is approximately 90% in both high and low loading cases. A cubic relationship between mass concentration and aerodynamic diameter suggests pellet emission particles, in both cases, are spherical (Fig. S4†), although the mode diameters increased when the fuel loading was reduced (76 nm for the high loading to 109 nm for the low loading). When pellet particle emissions were passed through the TD, effective density increased (Fig. S5†), suggesting the presence of a refractory component, *e.g.*, a BC core. Contrastingly, wood particles are 45–50% OM by mass with the remaining mass comprised of BC. Mode particle sizes (180–216 nm) of the wood particles were larger than for the pellet particles, irregularly shaped, and showed no mass or optical changes when thermally denuded. The irregular shape may contribute to overestimations of particle diameter as the SMPS measurement provides a measure of the mobility diameter. Further this overestimation is likely to propagate into the mass concentration calculation, however the effective density estimations should account somewhat for this over estimation.

## Optical properties of PM

AAE values (Fig. 1) for the pellet experiments were 3.1 ± 0.1 to 3.5 ± 0.4 and were always greater than one, indicating the presence of BrC that has a pronounced wavelength-dependent absorption. Particle effective densities increased and AAE decreased after passing the pellet emissions through a thermal denuder, suggesting a loss of the absorbing semi-volatile fraction and the presence of a refractory core, *e.g.*, consisting of BC, which was approximately ~10% of PM. The high pellet loading particle $MAC_{405}$ ($2.7 \pm 0.9$ $m^2$ $g^{-1}$) and $MAC_{781}$ ($0.3 \pm 0.1$ $m^2$ $g^{-1}$) are both a factor of five lower than the low pellet loading $MAC_{405}$ ($11.5 \pm 6.6$ $m^2$ $g^{-1}$) and $MAC_{781}$ ($1.4 \pm 0.7$ $m^2$ $g^{-1}$), suggest more absorbing, 'browner' particles are produced under the low pellet loading.

An AAE of 0.9 ± 0.1 for the birch emission particles and 1.0 ± 0.6 for the spruce particles indicate a lack of BrC compounds modifying typical BC absorption; however, brief periods of AAE >4.0 are observed when pollutant emissions are high, *e.g.*, on refuelling, suggesting the presence of BrC at those times when temperatures are lower and combustion is least efficient. The birch particle $MAC_{405}$ of $6.2 \pm 11.0$ $m^2$ $g^{-1}$ and $MAC_{781}$ of $3.1 \pm 5.1$ $m^2$ $g^{-1}$ are more similar to the pellet MACs, suggesting a similar level of absorption, but are an order of magnitude lower than for spruce particles, where $MAC_{405} = 33.8 \pm 27.4$ $m^2$ $g^{-1}$ and $MAC_{781} = 11.3 \pm 10.3$ $m^2$ $g^{-1}$ indicating more intense absorption. It is also clear the wood log MACs are much more variable, again in line with combustion cycles. PAHs form under similar conditions to BC, can be effectively absorbed by BC and contribute to BC formation through condensation[56,76] thus the concomitance of high $EF_{BC}$ and $EF_{PAH}$ in the spruce case is expected.

## OC speciation during FIGAERO sampling

Here we describe the speciated OC measurements made using the FIGAERO-ToF-CIMS. For the wood log experiments these descriptions represent transient measurements during a smaller portion of the entire wood cycle, see the Iodide FIGAERO-ToF-CIMS section of the methodology and the ESI† for details. This means that whilst the description of speciated OC from the pellet stove is representative of typical combustion, those for the wood logs should be considered transient. As such, comparisons of speciated OC EFs for the wood log emissions

are most appropriately compared with their corresponding transient non-speciated EFs (*i.e.*, OC, BC, THC *etc.*).

As described previously, for the wood log cycle averages, the MCE was lower for the spruce combustion compared to the birch. For the transient sampling, this distinction is amplified. The birch sampling occurs at an even greater MCE of 0.9938 ± 0.0035 whereas the spruce sampling occurs at an even lower MCE of 0.9615 ± 0.0218 when compared to the cycle averages. Correspondingly, the $EF_{OC}$ of the transient measurement during FIGAERO sampling is lower for the higher MCE birch case at 149 ± 77 mg $kg^{-1}$ or approximately 85% that of the average $EF_{OC}$. Further, the transient $EF_{OC}$ of 689 ± 1390 mg $kg^{-1}$ for the lower MCE spruce case is approximately 3.5 times greater than the cycle average. See Table 1 for comparisons of transient *vs.* average EFs.

For the pellet emission particles, the sum of speciated particulate OM measured by the FIGAERO-ToF-CIMS ($EF_{OM\_FIG\_par}$) was 29.0 ± 8.70 mg $kg^{-1}$ for the high loading and 65.7 ± 19.7 mg $kg^{-1}$ for the low loading (Table 1). $EF_{OM\_FIG\_par}$ for the wood log emissions was 46.1 ± 13.8 mg $kg^{-1}$ for the birch case and 81.5 ± 24.5 mg $kg^{-1}$ for the spruce case. These are of a comparable order of magnitude to the those of the pellet cases, although broadly, the lower MCE low pellet loading and spruce cases exhibit the higher $EF_{OM\_FIG\_par}$ compared to the higher MCE high pellet loading and birch cases.

For the pellet cases and the spruce case, approximately 10–13% of the OM is quantified by FIGAERO-ToF-CIMS but for the birch case this increases to 31%. This suggests the majority of the OM is comprised of compounds not readily detectable by FIGAERO-ToF-CIMS. This may be for several reasons. For example, some compounds are not detectable by iodide ionisation *e.g.* resin acids,[77] aliphatic compounds or other evaporites that have not combusted in the low temperature pellet cases. Additionally, some larger molecular weight compounds have lower volatilities than those accessible through filter evaporation as employed by the FIGAERO and thus remain unquantified. It may be that the high MCE and high temperatures of the birch combustion produces the greatest quantity of detectable compounds *e.g.*, more oxygenated and of lower molecular weights. Additionally, the combustion conditions between the birch and high pellet loading cases are different: the temperature of the log fire is greater, and the heterogeneity of the fuel in the chamber is greater, *e.g.* producing more pyrolytic conditions and thus more pyrolysis products.

As levoglucosan is a pyrolysis product and well-characterised BB tracer,[78] we describe its emission characteristics here as an example for the behaviour of an important semi-volatile species. Particle phase $EF_{Levoglucosan}$ for the high pellet load were 16.5 ± 4.9 mg $kg^{-1}$ and 24.6 ± 7.4 mg $kg^{-1}$ for the low pellet load, consistent with literature values.[75,78–81] This corresponds to 5% and 2% of PM respectively, which again agrees with the literature.[81–83] A particle phase $EF_{Levoglucosan}$ of 26.9 ± 8.1 mg $kg^{-1}$ for the birch case is comparable in magnitude to the low pellet loading. This is consistent with the descriptions of (a) combustion heterogeneity in the high MCE, high temperature birch case, and (b), the lower MCE, high $EF_{BC}$ description of the lower pellet loading case, both suggesting or indicating more pyrolytic conditions (see chemical composition of emission section). Moreover, the high temperature, low MCE spruce case presents the highest $EF_{Levoglucosan}$ of 49.4 ± 14.8 mg $kg^{-1}$, indicating these conditions are the most conducive for production of pyrolysis products. This is confirmed by the very high transient spruce case $EF_{BC}$ of 1260 ± 1716 mg $kg^{-1}$. This is further reflected in the wood cycle average $EF_{PAH}$ where 172 mg $kg^{-1}$ is measured for the spruce case compared to 4 mg $kg^{-1}$ for the high pellet loading, 7 mg $kg^{-1}$ for the low pellet loading and 17 mg $kg^{-1}$ for the birch case.

Levoglucosan is a pyrolysis product requiring high temperatures and low oxygen content for its formation. While some SMAs are formed in a similar manner, *e.g.* nitrocatechol, others, like vanillin, require an environment to which the pellet stove is optimised to ensure they are not combusted, *i.e.*, oxidative conditions and lower temperatures. The 19 SMAs (see Materials and methods) described in the literature (Table S1†) as BrC components[32,33,37,40,48,84] that were identified in this work contributed 1.4% by mass of OM for the high pellet loading and 1.8% for the low pellet loading. Sum particle phase EFs ($EF_{SMA\_par}$) were 3.12 ± 0.94 mg $kg^{-1}$ for the high pellet loading and 11.8 ± 3.60 mg $kg^{-1}$ for the low pellet loading. When compared with their equivalent MCE wood log counterparts, these are an order of magnitude greater, *cf.* the high pellet loading $EF_{SMA\_par}$ with the birch case, where $EF_{SMA\_par} = 0.61 \pm 0.18$ mg $kg^{-1}$, and the low pellet loading with $EF_{SMA\_par} = 2.28 \pm 0.69$ mg $kg^{-1}$ for the spruce case. One explanation may be a greater proportion of SMAs do not combust in the pellet stove and so can survive to be emitted. This anecdotally agrees with lower pellet stove chimney bottom temperatures of 100 °C–150 °C compared to the wood burning stove. This explanation is predicated on the assumption that chimney bottom temperature is an accurate proxy for combustion chamber temperature, which may not be the case if heat transfer from the combustion chamber is very efficient and minimal heat is lost through the chimney.

The speciation of the organic fraction is substantially different between appliances, at similar OC emissions, likely caused by the differences in MCE, combustion temperature and fuel heterogeneities in the combustion chamber. The low temperature pellet emissions preserve a greater quantity of SMAs compared to the high temperature wood log cases. Lowering the pellet loading causes more pyrolysis, increasing BC, PAHs and levoglucosan, but also reduces temperatures, preserving more OC as well as SMAs. The high MCE birch case is still susceptible to fuel and temperature heterogeneities in the combustion chamber causing an increase in BC, PAH and levoglucosan, exacerbated by higher temperatures, which also combusts the SMAs. The spruce case had high temperatures and low MCEs again with heterogeneities in the combustion chamber, which produces the largest quantities of BC, PAH and levoglucosan.

### Reconciling chemical and optical properties

The particle emissions from the high pellet loading case were OC rich and contained light absorbing PAHs and SMAs in

similar quantities. These particles had a high AAE suggesting the presence of BrC, although low MACs suggest weak absorption. For the low pellet loading case, particles are also OC rich with a similar AAE to the high loading, but MACs were greater by a factor of 4.5. This agrees with larger EFs of SMA and PAHs, which increased by a factor of four and two respectively. Additionally, EFs of THC, PM, BC and OC all increased, indicating that lowering the fuel loading of the pellet stove increases both absolute particle and gas emissions in addition to increasing wavelength-dependent particle optical absorption producing 'browner' particles.

For the wood cases, AAEs equal to one indicate a lack of wavelength dependence on absorption and thus a lack of BrC, which reconciles with low $EF_{SMA}$. Additionally, MACs for the birch emissions were of a comparable order to the pellet emissions, indicating weak absorption. Any absorption is then attributed to the BC, of which, little was measured during FIGAERO sampling. MACs for the spruce emissions were an order of magnitude greater than for the birch, suggesting much stronger absorption, which is attributable to the order of magnitude increase in $EF_{BC}$. Although PAHs were measured for the wood emissions, they represent cycle averages and are difficult to compare with the transient OC, BC and SMA EFs and transient optical measurements discussed here. However, PAHs emissions were clearly greater from the wood cases compared to the pellets, but not so great as to modify the dominance of BC on the optical absorption.

## Atmospheric impacts

To illustrate the implications of the emission factors derived in this study on potential air pollution burdens, we devised a simple scenario where a generic, current energy consumption, of a national scale, for these two appliances are exchanged to represent a move away from wood log stove technology to pellet stove technology. The aim of this exercise is to contextualise our results as burdens, leveraging the in-depth, molecularly resolved and phase resolved characterization of speciated emission factors (Table 2, see the Generalised national burdens scenario section for details). The aim of this exercise is not to present accurate or representative emission factors for these appliances, *e.g.*, for use in detailed assessments at a policy level, but rather to demonstrate the potential impacts these molecularly and phase resolved organic EFs could translate to, as national burdens. It is further noted that the EFs derived here refer to these individual appliances only and should not be taken as general EFs for these appliance types.

Given the assumed energy demand distribution here, the PM burden was 0.329 kt, the BC burden was 0.119 kt and the OC burden was 0.084 kt. Swapping demand resulted in a PM reduction of 12% to 0.300 kt and a BC reduction of 42% to 0.041 kt. Additionally, the particulate PAH burden reduced considerably by 84% from 13.37 t to 2.03 t. In contrast was an increase of OC to 0.132 kt, or 57%. However, the sum of OC speciated compounds (particle phase FIGAERO organics) reduce by 20% from 22.8 t to 18.1 t. For the gas phase FIGAERO organics, there was instead an increase from 5.1 t to 13.7 t (268%), shifting much of the particle mass savings to the gas phase. In line with the decrease in particle phase FIGAERO organics is the decrease in the levoglucosan burden by 27% from 13.3 t to 9.7 t. Once again there is an increase in corresponding gaseous emissions, from 0.09 t to 0.24 t (267%).

Unlike the FIGAERO organics and levoglucosan, the SMA burden increases in both particle (0.55 t to 2.00 t, 364%) and gas phases (0.47 t to 2.63 t, 560%). Despite these large relative increases, the absolute total mass of the SMAs is still small compared to other classes of organic compounds, however the health impacts of this magnitude increase are uncertain. An additional uncertainty is how important this increase might be, considering the reduction of other deleterious material such as the PAHs.

From this exercise, two points become clear. Firstly, the comparison of emissions from the two stoves in this study shows that the pellet stove was a greater source of at least some classes of organic carbon that are relevant to climate processes and health, *i.e.* the SMAs. This is also evident from the reported EFs (on both a per fuel mass and per useful energy delivered basis). Secondly, even if particle phase emissions were decreased, corresponding gas phase emissions could increase, in part, offsetting the total reduction of a pollutant. Shifting the distribution of a pollutant from the particle to gas phase is likely to increase the propensity for secondary chemistry later on, which could further impact climatic and health effects. This highlights the issue of shifting a primary pollution issue into a secondary pollution issue and the need for further studies to quantify the particle burdens from POA and precursors of SOA.

This study also highlights the importance of simultaneous gas and particle measurements to accurately quantify total,

Table 2 Scenarios of emission burdens. Hypothetical national scale current energy demands from the wood-burning appliances are contrasted with a swapped energy demand scenario

| Scenario | Appliance | Energy consumption (PJ) | BC (kt) | OC (kt) | PM (kt) | THC (kt) | PAHs (t) | FIGAERO organics particle (gas) (t) | Levoglucosan particle (gas) (t) | Literature. SMAs particle (gas) (t) |
|---|---|---|---|---|---|---|---|---|---|---|
| Current | Pellet | 0.7 | 0.003 | 0.013 | 0.027 | 0.059 | 0.07 | 1.59 (1.33) | 0.84 (0.02) | 0.20 (0.26) |
| | Wood | 7.0 | 0.116 | 0.071 | 0.302 | 0.652 | 13.3 | 21.2 (3.78) | 12.4 (0.06) | 0.35 (0.21) |
| | Total | 7.7 | 0.119 | 0.084 | 0.329 | 0.711 | 13.4 | 22.8 (5.11) | 13.3 (0.09) | 0.55 (0.47) |
| Swapped | Pellet | 7.0 | 0.029 | 0.125 | 0.270 | 0.592 | 0.70 | 15.9 (13.3) | 8.45 (0.23) | 1.97 (2.6) |
| | Wood | 0.7 | 0.012 | 0.007 | 0.030 | 0.065 | 1.33 | 2.12 (0.38) | 1.24 (0.01) | 0.04 (0.02) |
| | Total | 7.7 | 0.041 | 0.132 | 0.300 | 0.657 | 2.03 | 18.01 (13.7) | 9.69 (0.24) | 2.00 (2.63) |
| Total | Current-swapped | | −0.078 | 0.049 | −0.029 | −0.054 | −11.3 | −4.73 (8.58) | −3.59 (0.15) | 1.45 (2.16) |

rather than just particle phase, organic emissions from RWC appliances. Furthermore, for an extended study covering a larger range of available appliances, *e.g.*, linked to emission inventories, there may be many benefits to applying this methodology to assess the effectiveness of, for example, appliance swap schemes, or policies that aim to transition to technologies where the gas phase component of emission might be significant.

## Conclusions

Carbonaceous particulate and gaseous emissions from a wood burning stove and a pellet stove have been quantified, contrasted and characterised under laboratory conditions. This includes online analysis of particle morphological, chemical and optical properties using state-of-the-art instrumentation. Emissions from the wood log burning stove during periods of high and low combustion efficiency were compared with a pellet boiler operated under high and low fuel loadings. EFs of BC and OC were derived using a PASS-3 and SMPS. Speciated gas and particle phase EFs of mono-substituted aromatic compounds were made using a FIGAERO-ToF-CIMS and measurements of PAHs were made using a GC-MS.

For both appliances, periods of high MCE were characterised by high emissions of $CO_2$ and low emissions of particles and other gases. Average particle mass loadings from the pellet stove were lower than the wood-burning stove, although, under low loadings, the pellet stove emitted a larger concentration of particle mass than efficient wood burning, including a significant OC fraction.

Although mass concentrations were highly variable between the operational modes of the two appliances, the physicochemical properties of the particles were distinct to each appliance. The pellet particles were spherical, approximately 10% BC and approximately 90% optically absorbing OM (BrC) by mass. Contrastingly, the wood log particles were larger and mainly amorphous BC accounting for approximately 50% of PM mass.

The optically active components of the OC rich pellet particle emissions were a mixture of PAHs and SMAs. Sum $EF_{SMA}$ were up to an order of magnitude greater in the pellet cases than for the wood log emissions. Decreasing the fuel loading of the pellet stove decreased the MCE. Correspondingly, BC EFs increased by a factor of six, OM EFs by a factor of five as well as the optical absorption (MAC) of the material by a factor of four to five, caused by an increase in EFs of SMAs by a factor of four and PAHs by a factor of two. Thus running the pellet boiler under reduced fuel loadings produced more particles and 'browner' particles.

Optical absorption from birch emission particles at a high MCE was of a comparable magnitude to the pellets, although no BrC was present. The spruce particle emissions measured at low MCE indicate much stronger absorption than the high MCE birch particle emissions. This absorption was likely dominated by high emissions of BC. PAH emissions from the low MCE spruce particle emissions were ten times greater than the next highest emission from the high MCE birch particles and 100 to 200 times greater than those measured from the pellet stove.

To contextualise the impact of the EFs, the impact of swapping energy demands between the wood log stove and the pellet stove tested in this study was estimated at a national scale using a hypothetical pollution burden analysis scenario. This hypothetical pollution burden analysis is specific to the individual appliances studied here, as well as the conditions under which they were operated, meaning these results are not necessarily representative of the appliance types in general, or their true usage in the field. Reductions of 12% for PM and 42% for BC were somewhat offset by an increase in OC of 57%. The effect on speciated organic compounds were more nuanced. For example, total concentrations of key compounds decreased, such as the major product levoglucosan, whereas others, such as the SMAs, increased. Irrespective of how the total burden of speciated organics change, gas phase burdens always increased. This illustrates one of the major challenges in emissions characterisation of organic compounds: that shifting particle phase material into the gas phase *via* phase partitioning can obscure true reductions in total material emitted, and also provide delayed particulate pollution if the gas phase emissions are precursors to subsequent SOA formation. As such, future work should investigate representations of phase partitioned semi-volatile organic compounds from polluting emission sources. Additionally, more accurate assessments of national emissions considering gas and particle phase emissions are needed to better understand the true effectiveness of abatement policies on pollutant reduction. Investigating the SOA formation potential from shifting emissions into the gas phase should also be investigated in greater detail, as this might have ramifications for transporting delayed particle pollution away from source regions.

## Author contributions

MP: writing – original draft, review & editing, visualization, investigation, data curation, formal analysis. XK: writing – review & editing, methodology, investigation, data curation, formal analysis. XP: investigation, data curation, formal analysis. JH: investigation. DB: resources, data curation, investigation. RP: conceptualization, methodology, project administration. JP: funding acquisition, conceptualization, methodology, project administration. MH writing – review & editing, conceptualization, methodology, project administration.

## Conflicts of interest

There are no conflicts to declare.

## Acknowledgements

The research presented is a contribution to the Swedish Strategic Research Area Modelling the Regional and Global Earth System (MERGE). The authors would like to thank Harald Stark and Archit Mehra for their help implementing the voltage

scanning features of the ToF-CIMS. This work was supported by Energimyndigheten (Swedish Energy Agency) Project No. 44702-1, the Swedish Research Council (Grant 2018-04430), Formas (Grant 2019-00586) and VR Project No. 2015-04123. X. K. acknowledges support from the Swedish Foundation for International Cooperation in Research and Higher Education (CH2019-8361).



## References

1 CrossBorder Bioenergy, *EU Handbook – Small Scale Heating Markets*, 2012.
2 EU, *Directive 2018/2001 of the European Parliament and of the Council on the Promotion of the Use of Energy from Renewable Sources*, 2018.
3 EU, *Directive 2009/28/EC of the European Parliament and of the Council on the Promotion of the Use of Energy from Renewable Sources and Amending and Subsequently Repealing Directives 2001/77/EC and 2003/30/EC*, 2008, vol. 1.
4 R. Matthews, N. Mortimer, J. P. Lesschen, T. J. Lindroos, L. Sokka, A. Morris, P. Henshall, C. Hatto, O. Mwabonje, J. Rix, E. Mackie and M. Sayce, *Carbon impacts of biomass consumed in the EU: quantitative assessment Final report, project: DG ENER/C1/427 Part A: Main Report*, 2015.
5 European Commission, *Green Paper - A 2030 Framework for Climate and Energy Policies*, 2013.
6 G. W. Fuller, A. H. Tremper, T. D. Baker, K. E. Yttri and D. Butterfield, *Atmos. Environ.*, 2014, **87**, 87–94.
7 C. Lin, R. J. Huang, D. Ceburnis, P. Buckley, J. Preissler, J. Wenger, M. Rinaldi, M. C. Facchini, C. O'Dowd and J. Ovadnevaite, *Nat. Sustain.*, 2018, **1**, 512–517.
8 C. Lin, D. Ceburnis, R. J. Huang, W. Xu, T. Spohn, D. Martin, P. Buckley, J. Wenger, S. Hellebust, M. Rinaldi, M. Cristina Facchini, C. O'Dowd and J. Ovadnevaite, *Atmos. Chem. Phys.*, 2019, **19**, 14091–14106.
9 World Health Organization, *Residentail Heating with Wood and Coal: Health Impacts and Policy Options in Europe and North America*, Copanhagen, 2014.
10 T. Sigsgaard, B. Forsberg, I. Annesi-Maesano, A. Blomberg, A. Bølling, C. Boman, J. Bønløkke, M. Brauer, N. Bruce, M. E. Héroux, M. R. Hirvonen, F. Kelly, N. Künzli, B. Lundbäck, H. Moshammer, C. Noonan, J. Pagels, G. Sallsten, J. P. Sculier and B. Brunekreef, *Eur. Respir. J.*, 2015, **46**, 1577–1588.
11 Y. Olsen, J. K. Nøjgaard, H. R. Olesen, J. Brandt, T. Sigsgaard, S. C. Pryor, T. Ancelet, M. del M. Viana, X. Querol and O. Hertel, *Atmos. Pollut. Res.*, 2020, **11**, 234–251.
12 European Pellet Council, *European Biomass Association Statistical Report - European Bioenergy Outlook: Pellet Market Overview*, Brussels, 2017.
13 W. M. Champion and A. P. Grieshop, *Environ. Sci. Technol.*, 2019, **53**, 6570–6579.
14 R. Mack, H. Hartmann, C. Mandl, I. Schüßler, F. Volz, J. Furborg and J. B. Illerup, *General rights Development of Next Generation and Clean Wood Stoves-Final project report Development of Next Generation and Clean Wood Stoves-Final project report*, 2018.
15 J. C. Corbin, A. Keller, U. Lohmann, H. Burtscher, B. Sierau and A. A. Mensah, *Aerosol Sci. Technol.*, 2015, **49**, 1037–1050.
16 Y. Olsen, J. K. Nøjgaard, H. R. Olesen, J. Brandt, T. Sigsgaard, S. C. Pryor, T. Ancelet, M. del M. Viana, X. Querol and O. Hertel, *Atmos. Pollut. Res.*, 2020, **11**, 234–251.
17 M. Amann, J. Cofala, Z. Klimon, C. Nagl and W. Schieder, *Measures To Address Air Pollution From Small Combustion Sources*, 2018.
18 M. O. Andreae and A. Gelencsér, *Atmos. Chem. Phys.*, 2006, **6**, 3131–3148.
19 R. P. Pokhrel, E. R. Beamesderfer, N. L. Wagner, J. M. Langridge, D. A. Lack, T. Jayarathne, E. A. Stone, C. E. Stockwell, R. J. Yokelson and S. M. Murphy, *Atmos. Chem. Phys.*, 2017, **17**, 5063–5078.
20 D. A. Lack and C. D. Cappa, *Atmos. Chem. Phys.*, 2010, **10**, 4207–4220.
21 S. Liu, A. C. Aiken, K. Gorkowski, M. K. Dubey, C. D. Cappa, L. R. Williams, S. C. Herndon, P. Massoli, E. C. Fortner, P. S. Chhabra, W. A. Brooks, T. B. Onasch, J. T. Jayne, D. R. Worsnop, S. China, N. Sharma, C. Mazzoleni, L. Xu, N. L. Ng, D. Liu, J. D. Allan, J. D. Lee, Z. L. Fleming, C. Mohr, P. Zotter, S. Szidat and A. S. H. Prévôt, *Nat. Commun.*, 2015, **6**, 8435.
22 H. Lukács, A. Gelencsér, S. Hammer, H. Puxbaum, C. A. Pio, M. Legrand, A. Kasper-Giebl, M. Handler, A. Limbeck, D. Simpson and S. Preunkert, *J. Geophys. Res. Atmos.*, 2007, **112**, 1–9.
23 E. Liakakou, D. G. Kaskaoutis, G. Grivas, I. Stavroulas, M. Tsagkaraki, D. Paraskevopoulou, A. Bougiatioti, U. C. Dumka, E. Gerasopoulos and N. Mihalopoulos, *Sci. Total Environ.*, 2020, **708**, 135019.
24 Y. Zhang, A. Albinet, J.-E. Petit, V. Jacob, F. Chevrier, G. Gille, S. Pontet, E. Chrétien, M. Dominik-Sègue, G. Levigoureux, G. Močnik, V. Gros, J.-L. Jaffrezo and O. Favez, *Sci. Total Environ.*, 2020, **743**, 140752.
25 L. Zhang, Z. Luo, W. Du, G. Li, G. Shen, H. Cheng and S. Tao, *Environ. Pollut.*, 2020, **267**, 115652.
26 N. K. Kumar, J. C. Corbin, E. A. Bruns, D. Massabó, J. G. Slowik, L. Drinovec, G. Močnik, P. Prati, A. Vlachou, U. Baltensperger, M. Gysel, I. El-Haddad and A. S. H. Prévôt, *Atmos. Chem. Phys.*, 2018, **18**, 17843–17861.
27 C. Li, Q. He, A. P. S. Hettiyadura, U. Käfer, G. Shmul, D. Meidan, R. Zimmermann, S. S. Brown, C. George, A. Laskin and Y. Rudich, *Environ. Sci. Technol.*, 2020, **54**, 1395–1405.
28 A. Zhang, Y. Wang, Y. Zhang, R. J. Weber, Y. Song, Z. Ke and Y. Zou, *Atmos. Chem. Phys.*, 2019, 1–36.
29 H. Brown, X. Liu, Y. Feng, Y. Jiang, M. Wu, Z. Lu, C. Wu, S. Murphy and R. Pokhrel, *Atmos. Chem. Phys.*, 2018, **18**, 17745–17768.
30 V. Samburova, J. Connolly, M. Gyawali, R. L. N. Yatavelli, A. C. Watts, R. K. Chakrabarty, B. Zielinska, H. Moosmüller and A. Khlystov, *Sci. Total Environ.*, 2016, **568**, 391–401.
31 Z. Kitanovski, J. Hovorka, J. Kuta, C. Leoni, R. Prokeš, O. Sáňka, P. Shahpoury and G. Lammel, *Environ. Sci. Pollut. Res.*, 2021, **28**, 59131–59140.

32 P. Lin, J. Liu, J. E. Shilling, S. M. Kathmann, J. Laskin and A. Laskin, *Phys. Chem. Chem. Phys.*, 2015, **17**, 23312–23325.
33 L. T. Fleming, P. Lin, J. M. Roberts, V. Selimovic, R. Yokelson, J. Laskin, A. Laskin and S. A. Nizkorodov, *Atmos. Chem. Phys.*, 2020, **20**, 1105–1129.
34 E. Reyes-Villegas, M. Priestley, Y. C. Ting, S. Haslett, T. Bannan, M. Le Breton, P. I. Williams, A. Bacak, M. J. Flynn, H. Coe, C. Percival and J. D. Allan, *Atmos. Chem. Phys.*, 2018, **18**, 4093–4111.
35 L. E. Hatch, W. Luo, J. F. Pankow, R. J. Yokelson, C. E. Stockwell and K. C. Barsanti, *Atmos. Chem. Phys.*, 2015, **15**, 1865–1899.
36 K. Sekimoto, A. R. Koss, J. B. Gilman, V. Selimovic, M. M. Coggon, K. J. Zarzana, B. Yuan, B. M. Lerner, S. S. Brown, C. Warneke, R. J. Yokelson, J. M. Roberts and J. de Gouw, *Atmos. Chem. Phys.*, 2018, **18**, 9263–9281.
37 C. Mohr, F. D. Lopez-Hilfiker, P. Zotter, A. S. H. Prévôt, L. Xu, N. L. Ng, S. C. Herndon, L. R. Williams, J. P. Franklin, M. S. Zahniser, D. R. Worsnop, W. B. Knighton, A. C. Aiken, K. J. Gorkowski, M. K. Dubey, J. D. Allan, J. A. Thornton, A. S. H. Prévoît, L. Xu, N. L. Ng, S. C. Herndon, L. R. Williams, J. P. Franklin, M. S. Zahniser, D. R. Worsnop, W. B. Knighton, A. C. Aiken, K. J. Gorkowski, M. K. Dubey, J. D. Allan and J. A. Thornton, *Environ. Sci. Technol.*, 2013, **47**, 6316–6324.
38 C. J. Gaston, F. D. Lopez-Hilfiker, L. E. Whybrew, O. Hadley, F. McNair, H. Gao, D. A. Jaffe and J. A. Thornton, *Atmos. Environ.*, 2016, **138**, 99–107.
39 C. M. G. Salvador, R. Tang, M. Priestley, L. Li, E. Tsiligiannis, M. Le Breton, W. Zhu, L. Zeng, H. Wang, Y. Yu, M. Hu, S. Guo and M. Hallquist, *Atmos. Chem. Phys.*, 2021, **21**, 1389–1406.
40 X. Kong, C. M. Salvador, S. Carlsson, R. Pathak, K. O. Davidsson, M. Le Breton, S. M. Gaita, K. Mitra, Å. M. Hallquist, M. Hallquist and J. B. C. Pettersson, *Sci. Total Environ.*, 2021, **754**, 142143.
41 F. D. Lopez-Hilfiker, C. Mohr, M. Ehn, F. Rubach, E. Kleist, J. Wildt, T. F. Mentel, A. Lutz, M. Hallquist and D. Worsnop, *Atmos. Meas. Tech.*, 2014, **7**, 983–1001.
42 A. Mehra, M. Canagaratna, T. J. Bannan, S. D. Worrall, A. Bacak, M. Priestley, D. Liu, J. Zhao, W. Xu, Y. Sun, J. F. Hamilton, F. A. Squires, J. Lee, D. J. Bryant, J. R. Hopkins, A. Elzein, S. H. Budisulistiorini, X. Cheng, Q. Chen, Y. Wang, L. Wang, H. Stark, J. E. Krechmer, J. Brean, E. Slater, L. Whalley, D. Heard, B. Ouyang, W. J. F. Acton, C. N. Hewitt, X. Wang, P. Fu, J. Jayne, D. Worsnop, J. Allan, C. Percival and H. Coe, *Faraday Discuss.*, 2021, **226**, 382–408.
43 H. Jiang, A. L. Frie, A. Lavi, J. Y. Chen, H. Zhang, R. Bahreini and Y. H. Lin, *Environ. Sci. Technol. Lett.*, 2019, **6**, 184–190.
44 B. H. Lee, F. D. Lopez-Hilfiker, C. Mohr, T. Kurtén, D. R. Worsnop, J. A. Thornton, T. Kurtén, D. R. Worsnop and J. A. Thornton, *Environ. Sci. Technol.*, 2014, **48**, 6309–6317.
45 Scandbio pellets, **https://www.scandbio.com/en/business-customer/our-products/pellets/**, accessed 8 February 2022.
46 H. Junninen, M. Ehn, T. Petäjä, L. Luosujärvi, T. Kotiaho, R. Kostiainen, U. Rohner, M. Gonin, K. Fuhrer, M. Kulmala, D. R. Worsnop, Petäjä, L. Luosujärvi, T. Kotiaho, R. Kostiainen, U. Rohner, M. Gonin, K. Fuhrer, M. Kulmala, D. R. Worsnop, T. Petäjä, L. Luosujärvi, T. Kotiaho, R. Kostiainen, U. Rohner, M. Gonin, K. Fuhrer, M. Kulmala and D. R. Worsnop, *Atmos. Meas. Tech.*, 2010, **3**, 1039–1053.
47 NS, *Norsk Standard NS 3058-1 Lukkede Vedfyrte Ildsteder Røykutslipp Del 1 : Prøvingsoppsett Og Fyringsmønster Enclosed Wood Heaters*, 1994.
48 A. Laskin, J. Laskin and S. A. Nizkorodov, *Chem. Rev.*, 2015, **115**, 4335–4382.
49 A. Mehra, Y. Wang, J. Krechmer, A. Lambe, F. Majluf, M. Morris, M. Priestley, T. Bannan, D. Bryant, K. Pereira, J. Hamilton, A. Rickard, M. Newland, H. Stark, P. Croteau, J. Jayne, D. Worsnop, M. Canagaratna, L. Wang and H. Coe, *Atmos. Chem. Phys.*, 2020, 1–24.
50 R. J. Yokelson, J. G. Goode, D. E. Ward, R. A. Susott, R. E. Babbitt, D. D. Wade, I. Bertschi, D. W. T. Griffith and W. M. Hao, *J. Geophys. Res.*, 1999, **104**, 30109–30125.
51 D. A. Lack, J. M. Langridge, R. Bahreini, C. D. Cappa, A. M. Middlebrook and J. P. Schwarz, *Proc. Natl. Acad. Sci. U. S. A.*, 2012, **109**, 14802–14807.
52 A. Rana, S. Dey, P. Rawat, A. Mukherjee, J. Mao, S. Jia, P. S. Khillare, A. K. Yadav and S. Sarkar, *Sci. Total Environ.*, 2020, **716**, 137102.
53 C. Liu, C. E. Chung, Y. Yin and M. Schnaiter, *Atmos. Chem. Phys.*, 2018, **18**, 6259–6273.
54 R. Bahadur, P. S. Praveen, Y. Xu and V. Ramanathan, *Proc. Natl. Acad. Sci. U. S. A.*, 2012, **109**, 17366–17371.
55 T. C. Bond and R. W. Bergstrom, *Aerosol Sci. Technol.*, 2006, **40**, 27–67.
56 B. Bessagnet and N. Allemand, *Review on Black Carbon (BC) and Polycyclic Aromatic Hydrocarbons (PAHs) Emission Reductions Induced by PM Emission Abatement Techniques*, Paris, 2020.
57 J. Zhai, X. Lu, L. Li, Q. Zhang, C. Zhang, H. Chen, X. Yang and J. Chen, *Atmos. Chem. Phys.*, 2017, **17**, 7481–7493.
58 B. J. Sumlin, C. R. Oxford, B. Seo, R. R. Pattison, B. J. Williams and R. K. Chakrabarty, *Environ. Sci. Technol.*, 2018, **52**, 3982–3989.
59 A. Bertrand, G. Stefenelli, E. A. Bruns, S. M. Pieber, B. Temime-Roussel, J. G. Slowik, A. S. H. Prévôt, H. Wortham, I. El Haddad and N. Marchand, *Atmos. Environ.*, 2017, **169**, 65–79.
60 A. Bougiatioti, I. Stavroulas, E. Kostenidou, P. Zarmpas, C. Theodosi, G. Kouvarakis, F. Canonaco, A. S. H. Prévôt, A. Nenes, S. N. Pandis and N. Mihalopoulos, *Atmos. Chem. Phys.*, 2014, **14**, 4793–4807.
61 S. Bau, B. Oury, V. Matera and X. Simon, *J. Phys. Conf. Ser.*, 2021, **1953**, 012004.
62 O. Sippula, K. Hytönen, J. Tissari, T. Raunemaa and J. Jokiniemi, *Energy Fuels*, 2007, **21**, 1151–1160.
63 E. A. Bruns, M. Krapf, J. Orasche, Y. Huang, R. Zimmermann, L. Drinovec, G. Močnik, I. El-Haddad, J. G. Slowik, J. Dommen, U. Baltensperger and A. S. H. Prévôt, *Atmos. Chem. Phys.*, 2015, **15**, 2825–2841.

64 A. A. Reda, H. Czech, J. Schnelle-Kreis, O. Sippula, J. Orasche, B. Weggler, G. Abbaszade, J. M. Arteaga-Salas, M. Kortelainen, J. Tissari, J. Jokiniemi, T. Streibel and R. Zimmermann, *Energy Fuels*, 2015, **29**, 3897–3907.
65 D. Bhattu, P. Zotter, J. Zhou, G. Stefenelli, F. Klein, A. Bertrand, B. Temime-Roussel, N. Marchand, J. G. Slowik, U. Baltensperger, A. S. H. Prévôt, T. Nussbaumer, I. El Haddad and J. Dommen, *Environ. Sci. Technol.*, 2019, **53**, 2209–2219.
66 M. O. Andreae and P. Merlet, *Global Biogeochem. Cycles*, 2001, **15**, 955–966.
67 P. Lehtikangas, *Lagringshandbok För Trädbränslen*, SLU, Sveriges lantbruksuniversitet, Uppsala, 1999.
68 K. Kindbom, T. Gustafsson, S. Åström, O.-K. Nielsen and K. Saarinen, *Potentials for Reducing the Health and Climate Impacts of Residential Biomass Combustion in the Nordic Countries*, 2018.
69 C. Schmidl, M. Luisser, E. Padouvas, L. Lasselsberger, M. Rzaca, C. Ramirez-Santa Cruz, M. Handler, G. Peng, H. Bauer and H. Puxbaum, *Atmos. Environ.*, 2011, **45**, 7443–7454.
70 E. A. Bruns, J. G. Slowik, I. El Haddad, D. Kilic, F. Klein, J. Dommen, B. Temime-Roussel, N. Marchand, U. Baltensperger and A. S. H. Prévôt, *Atmos. Chem. Phys.*, 2017, **17**, 705–720.
71 C. Alves, C. Gonçalves, A. P. Fernandes, L. Tarelho and C. Pio, *Res. Atmos.*, 2011, **101**, 692–700.
72 Y. Chen, C. Tian, Y. Feng, G. Zhi, J. Li and G. Zhang, *Atmos. Environ.*, 2015, **109**, 190–196.
73 N. K. Meyer, *Biomass Bioenergy*, 2012, **36**, 31–42.
74 A. Bertrand, G. Stefenelli, E. A. Bruns, S. M. Pieber, B. Temime-Roussel, J. G. Slowik, A. S. H. Prévôt, H. Wortham, I. El Haddad and N. Marchand, *Atmos. Environ.*, 2017, **169**, 65–79.
75 E. D. Vicente and C. A. Alves, *Res. Atmos.*, 2018, **199**, 159–185.
76 H. Omidvarborna, A. Kumar and D. S. Kim, *Renew. Sust. Energ. Rev.*, 2015, **48**, 635–647.
77 J. J. Schauer, M. J. Kleeman, G. R. Cass and B. R. T. Simoneit, *Environ. Sci. Technol.*, 2001, **35**, 1716–1728.
78 H. Bhattarai, E. Saikawa, X. Wan, H. Zhu, K. Ram, S. Gao, S. Kang, Q. Zhang, Y. Zhang, G. Wu, X. Wang, K. Kawamura, P. Fu and Z. Cong, *Res. Atmos.*, 2019, **220**, 20–33.
79 J. Sun, Z. Shen, Y. Zhang, Q. Zhang, F. Wang, T. Wang, X. Chang, Y. Lei, H. Xu, J. Cao, N. Zhang, S. Liu and X. Li, *Fuel*, 2019, **244**, 379–387.
80 E. D. Vicente, A. M. Vicente, M. Evtyugina, R. Carvalho, L. A. C. Tarelho, S. Paniagua, T. Nunes, M. Otero, L. F. Calvo and C. Alves, *Renewable Energy*, 2019, **140**, 319–329.
81 J. Sun, Z. Shen, Y. Zhang, Q. Zhang, Y. Lei, Y. Huang, X. Niu, H. Xu, J. Cao, S. S. H. Ho and X. Li, *Atmos. Environ.*, 2019, **205**, 36–45.
82 L. R. Mazzoleni, B. Zielinska and H. Moosmüller, *Environ. Sci. Technol.*, 2007, **41**, 2115–2122.
83 X. Sang-Arlt, H. Fu, Y. Zhang, X. Ding, X. Wang, Y. Zhou, L. Zou, G. F. Zellmer and G. Engling, *Atmosphere*, 2020, **11**, 1–14.
84 P. Lin, N. Bluvshtein, Y. Rudich, S. A. Nizkorodov, J. Laskin and A. Laskin, *Environ. Sci. Technol.*, 2017, **51**, 11561–11570.